



# DESIGN OF DYNAMIC VOLTAGE RESTORER TO ENHANCE POWER QUALITY RELYING ON RENEWABLE SOURCE

Haider M. Umran<sup>1</sup>

<sup>1</sup> MSc., University of Kerbala / College of Engineering / Electrical and Electronic Engineering Department, E-mail: [hyderumran@yahoo.com](mailto:hyderumran@yahoo.com)

<http://dx.doi.org/10.30572/2018/kje/090206>

## ABSTRACT

Power quality improvement of low voltage grid is a great challenge that confronts the sophisticated power applications, because their performance is highly sensitive to the quality of power supply. Dynamic Voltage Restorer (DVR) used widely as an efficient and skillful device to adjust electrical disturbances of the distribution grids. This paper introduces an overview of the components of the 3-phase dynamic voltage restorer and design its own control circuit. The performance of DVR was developed on the basis of the appropriate selection of Photovoltaic (PV) module instead of the present conventional designs. Through this design, the need of series converter (DVR) for the current from an electrical grid will end and the problems of power losses will curb. The PV-module is selected to meet the requirements of the DVR during voltage sag/swell on voltage line. The proposed system is mimicked in MATLAB software/Simulink and the findings are presented to prove the success of the design in terms of full congruence of the load voltage waveform with source voltage waveform, attaining 0.77% of THD analysis for the load voltage and the waveforms of PV system.

**KEYWORDS:** Power Quality, Renewable source, Distribution Grid, Dynamic Voltage Restorer (DVR), Buck Converter.

## 1. INTRODUCTION

Power quality is a crucial challenge for power station operators and their customers alike in a fiercely competitive work climate after exceeding the need for reliability. Critical loads are a product of evolution in the field of power system quality and the ability of those systems to provide the loads with fixed frequency, fixed sinusoidal wave and identical voltage with fixed RMS. Despite the progress of high quality standards, disturbances remain a major obstacle that cannot be avoided completely (Sanjay and Gaurav, 2013). So, the Dynamic Voltage Restorer (DVR) presents solution for the most common problems in the power distribution systems such as voltage sag/swell. The voltage sag is a decrease in the RMS nominal voltage level of (10-90%) for half cycle to one minute according to the definition of (IEEE-1159), which occurs due to a sudden disconnection of load or faults in the system. while the voltage swell is an increase in the RMS nominal voltage level to (110% - 180%) for the same duration of sag, which occurs due to a single line-to-ground fault [(Sanjay and Gaurav, 2013) and (Roger et. al., 2012)]. The DVR is a solid-state device which absorbs or injects voltage to the distribution grid autonomously to maintains the voltage in the load side in the record limits. It instates at the point of common coupling (PCC) between the distribution system and sensitive load, the basic components and location of DVR as illustrate in Fig. 1.

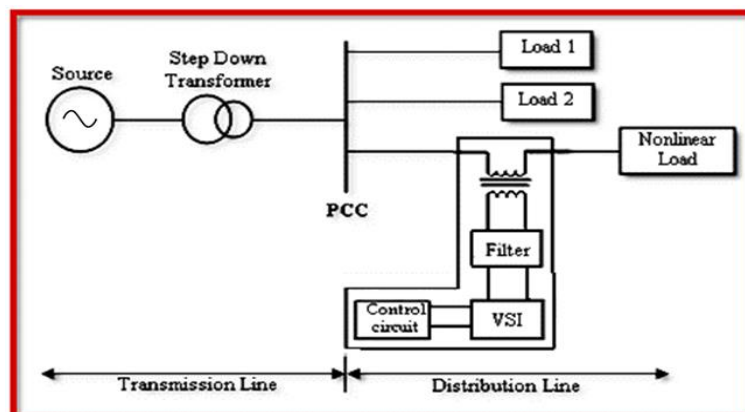


**Fig. 1. The basic components and location of DVR at distribution system.**

The DVR generally involves the voltage source inverter (VSI), injection transformer, harmonic filter, energy storage unit and control circuit. The function of (VSI) is converting the dc voltage that stored in energy storage unit to the line supply voltage after boosting the converted voltage across transformer. Capacity of energy storage unit (batteries) plays a major role to determine DVR ability on compensation. Control circuit employed to compare the voltage source with reference voltage to lead the switching signals of VSI and in result to inject the generated compensation voltage in DVR. There are some prevalent problems that associated with the

DVR action, such as; transient's emergence as a result to inject voltage with a load voltage during the voltages sag or swell and the power losses that arising from the battery charging across the transformer and VSI.

The DVR performance development has become target for researchers because of its ability to reduce the effect of voltage sags/ swells and their harsh impacts on consumers. So, many of the research have been done recently in the domain. (Yogita et al., 2016) described, analyzed and simulated the usefulness of Dynamic Voltage Restorer (DVR) for lessening the effect of voltage sag and swell due to three phase fault for IEEE 9-bus system. also, was used the programmable logic controller and other protection functions to implement the proposed DVR. (Kalaivani et al., 2016) evaluated the technical aspect feasibility which relate to use the dynamic voltage restorer with series injection transformer and analyzed the performance of DVR components by use MATLAB software. (Nagesh and Rajendra, 2016) discussed the basic component, the dynamic voltage restorer operating principle, and space vector pulse width modulation techniques that is used for controlling inverter. (Sanjay and Gaurang, 2015) proposed a novel control strategy to compensate the unbalance source voltage and current harmonics by using series active power filter in addition to simulate the proposed strategy by using the Matlab/Simulink. (Sathish, et al., 2015) proposed and simulated a control scheme to interrupt fault current for different fault cases at the downstream side of the DVR to improve power quality.

The drawback of the conventional DVR is considered as a high power loss device from the grid. Simulation model conducted in section (2) states the average current drawn from the busbar is (9.5 A/bus) to charge the battery. So, if a neighborhood has 13-bus radial system, then the total current drawn from the national grid is (123.5 A). This amount of current is exceedingly lossy for national grid efficiency. Another disadvantage of conventional DVR is that it requires the battery to be charged through a stage that converts AC/DC which is large in size, cost, and power consuming.

In this work, the improvement of power quality for distribution system was achieved based on the design of the DVR control circuit and selection of the Photovoltaic (PV) module. The photovoltaic array and battery designed independently to take into account the requirements of DVR. A switch mode dc power supply (Buck type) is employed to attain the Maximum Power Point Tracking (MPPT) for the (PV) based on Proportional and Integral (PI) controller. the system simulation results the DVR performance at up normal situation are appeared, the sag and swell voltages for line voltage.

The remainder of paper is arranged as follows: In section two, the reckoning of injection voltage according to the system equivalent circuit elucidated in details. Section three reviews the main parts of DVR and control circuit design for proposed system. Section four states selection of PV module and a design of MPPT unit. Section five implies a simulation of the suggested system by using Simulink power system, and result discussion that are obtained. Conclusions and important factors are stated in section six.

## 2. COMPUTATION OF INJECTION VOLTAGE

The Thevenin equivalent circuit for the grid with the DVR is illustrated in Fig. 2. The value of the system impedance ( $Z_{th}$ ) is determined by the type of fault that occurs in distributor. In case of unbalance voltage, the DVR will inject the required voltage to maintain voltage stability at load. When the voltage system ( $V_{th}$ ) drops, the voltage and power injected by the DVR can be calculated as follow:

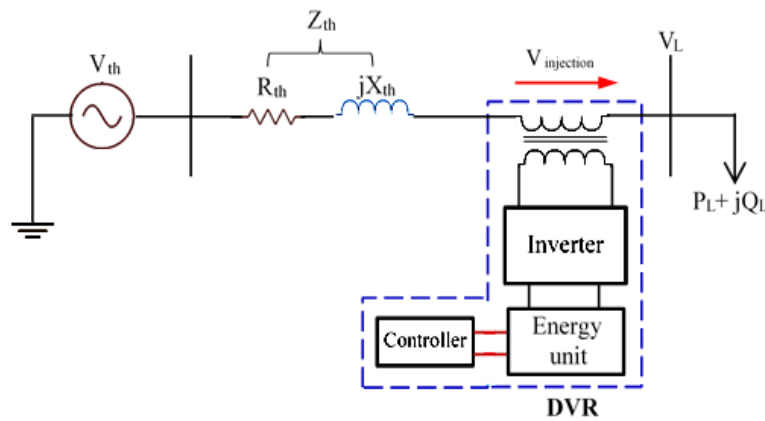


Fig. 2. The DVR equivalent circuit diagram.

With aid of Kirchoff's voltage law, the load voltage ( $V_L$ ) can calculate as:

$$V_L = V_{th} - Z_{th} I_L + V_{inj} \tag{1}$$

Now, the series voltage that injected by the DVR ( $V_{inj}$ ) calculates as:

$$V_{inj} = V_L + Z_{th} I_L - V_{th} \tag{2}$$

$$\text{And, } I_L = \left[ \frac{P_L + jQ_L}{V_L} \right] \tag{3}$$

Where,  $V_{th}$  the system voltage,  $I_L$  the load current, and  $(P_L, jQ_L)$  are active and reactive load power respectively. The load voltage is handled as a reference voltage hence the phase angle should be  $0^\circ$ , eq. (2) can be written in another way as:

$$V_{inj} \angle \alpha = V_L \angle 0 + Z_{th} I_L \angle (\beta - \theta) - V_{th} \angle \delta \tag{4}$$

Now, the power factor angle ( $\theta$ ) of load calculates is:

$$\theta = \tan^{-1} \left( \frac{Q_L}{P_L} \right) \quad 5$$

Now, the apparent power injected by the DVR is:

$$S_{DVR} = V_{inj.} \times I_L \quad 6$$

Consequently, the DVR capable of generating the necessary reactive power depending on disturbance conditions of power supply. Where,  $\alpha$  is the angle of the series injected of voltage ( $V_{inj.}$ ),  $\beta$  is the angle of system equivalent impedance,  $\delta$  is the angle of voltage system (angle between source and load voltages).

### 3. PARTS REVIEW OF THE DVR

The DVR is a power device designed to protect the nonlinear loads from most types of power supply side disturbances, it contains many of components, such as:

#### 3.1. Series Injection Transformer

The series injection transformer has three core tasks. It links up the distribution system with the VSI, raises the voltage simultaneously and compatibly with the source, and isolates the load from the DVR. Three single-phase transformers adopted to inject the missing voltage. The parameters of the injection transformer such as, the power rating, the turn-ratio, the ratings of voltage and current for the primary side, and the impedance values are most influential elements in degrading the DVR performance [(Shilpashinde and Kelapure, 2016) and (Dawn and Samina, 2016)], in addition to leakage inductance which must be at minimum to reduce the voltage drop at the transformer terminals.

#### 3.2. Voltage Source Inverter (VSI)

The VSI is used to produce a sinusoidal voltage at any required phase angle, frequency, and for any voltage magnitude. A three-phase full-bridge inverter, "Insulated Gate Bipolar Transistors (IGBT)" with PWM technique is adopted in this research. The benefit of using the Pulse-Width Modulation (PWM) includes, a high switching speed of the power switches which is characterized as simple and possess a rapid response (Prachi and Gaurav, 2013). Efficiency of VSI can be improved by increasing the switching frequency without increasing switching losses.

### 3.3. Control Circuit Design

The core objective of control circuit design is to maintain the voltage value constant thus protecting loads from disturbance conditions of power supply. This goal can be achieved by using Synchronized Pulse Width Modulation (SPWM) technique. A reference voltage (triangle signal) can be generated by integration of the adopted system frequency with the value of source voltage, to obtain balanced three-phase voltage without distortion. The reference voltage signal will compare with the (RMS) voltage that measured at the load side, to obtain an error signal and then generate the drive signals to the inverter switches [(Prachi and Gaurav, 2013) and (Apinan and Worawat, 2008)]. Therefore, the generated signal by the (PWM) will be identical in every cycle with the reference signal without change in the frequency, therefore; the output voltage is positively constant. This method provides that the output voltage is controlled without any extra components and with least harmonics. The control circuit that adopted in this paper is illustrated in the Fig. 3.

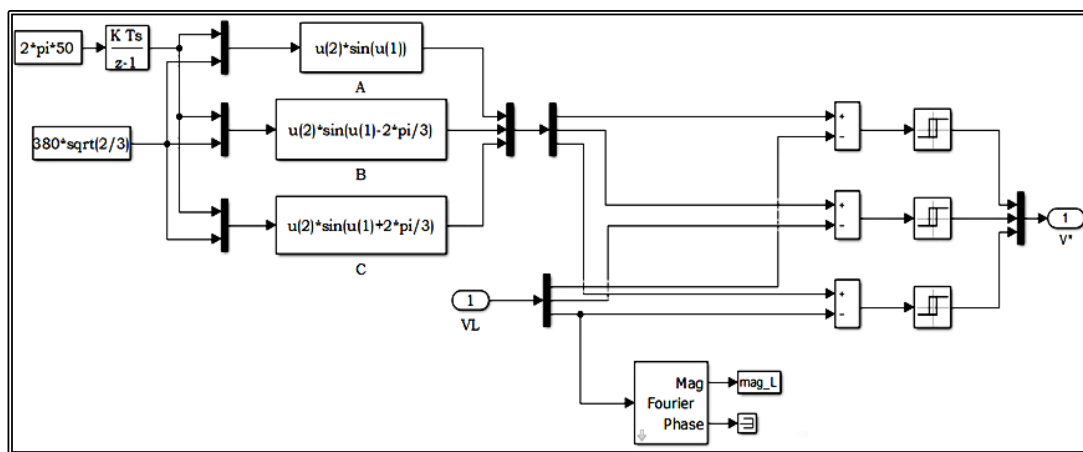
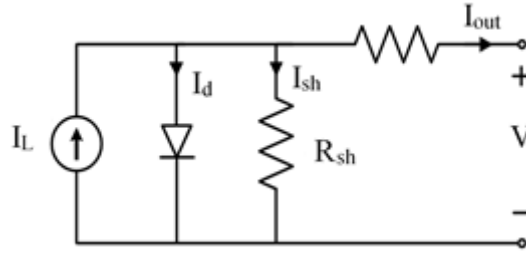


Fig. 3. The arrangement of approved control circuit.

## 4. PHOTOVOLTAIC DESIGN

The PV arrays are selected to meet the requirements of the DVR. The PV system will provide the DVR and battery by necessary voltage independently of power line. The solar module which adopted in this design is CS6X-310P (Sangita and Mini, 2014). The equivalent electrical circuit of PV-cell is illustrated in Fig. 4.

The PV characteristic equation which used to find each of the output voltage and current is (Canadian Solar Inc., 2016).



**Fig. 4. The equivalent circuit of PV cell.**

$$I_{out} = I_L - I_0 \left[ \exp\left(\frac{q(V + I_{out} \cdot R_s)}{KT}\right) - 1 \right] - \frac{V + I_{out} \cdot R_s}{R_{sh}} \quad 7$$

Where,  $I_{out}$  the output current of PV-cell,  $I_L$  the light generated current,  $I_0$  the diode saturation current,  $q$  the electron charge ( $1.6 \times 10^{-19}$  C),  $K$  the Boltzman constant ( $1.38 \times 10^{-23}$  J/K),  $T$  the cell temperature in Kelvin,  $V$  output voltage, and  $R_s$  and  $R_{sh}$  series and shunt resistances for the solar cell. The electrical characteristics of the solar panel that exploited in this work are included in [Table 1](#).

**Table 1. Characteristics of solar panel.**

Parameters	Maximum Power $P_{max}$	Voltage at Maximum Power Point $V_{MPP}$	Current at Maximum Power Point $P_{MPP}$	Short circuit current	Open circuit voltage
<b>Value</b>	310W	36.4V	8.52A	9.08A	44.9V

The design involves 21 modules connected in series. The Power –Voltage and Current–Voltage (P-V and I-V) characteristics of the cell under solar irradiation of ( $1000 \text{ W/m}^2$  and with temperature  $25^\circ\text{C}$ ), is illustrated in [Fig. 5](#).

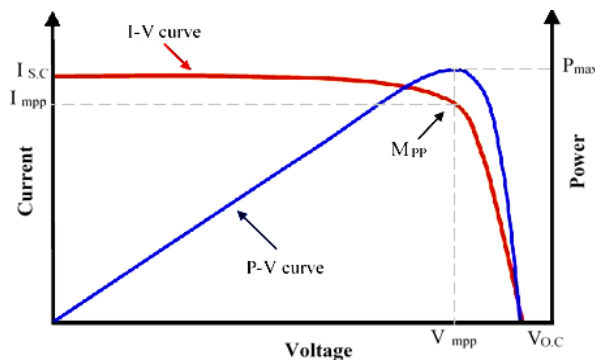


**Fig. 5. (P-V and I-V) of solar cell characteristics.**

It is worth mentioning; solar cell has quite low efficiency, therefore; the method of a maximum power point tracking (MPPT) is applied to raise the efficiency of cell power generation. In general, there is a single point on the curve of (V-P or V-I) known by MPP must be come true

to operate the PV system with high efficiency and with the maximum power output (Chandani and Jain, 2014; Saravana and Pratap, 2016). There are numerous algorithms of MPPT used to achieve this task, but this paper adopts a controller based on Proportional and Integral (PI). The system also involves solar panels, switch mode dc power supply (Buck converter type) and storage unit (battery).

#### 4.1. Buck Converter

The (dc to dc) converters were used in the PV system as an interface between the load and the PV module as well as transferring the maximum power from the solar PV module to the load. The load impedance is matched to the source impedance by changing the duty cycle of the converter to achieve the maximum power from the PV panel (Dinesh et. al., 2015). The basic arrangement of the step- down (buck) converter is illustrated in Fig. 6.

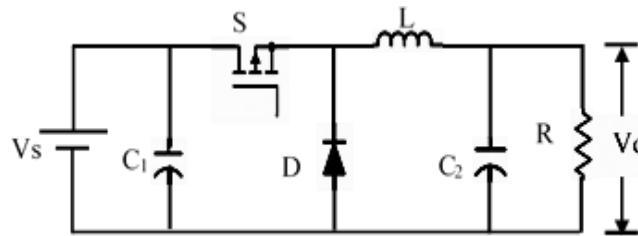


Fig. 6. Basic arrangement of buck converter.

The buck converter includes controlled switch (S) and diode (D). The buck converter has an inductor/capacitor (L and C<sub>2</sub>) filter at the output side to provide the continuous smooth output current to the load. Because the input current is directly applied to (S) and it has a highly dynamic waveform, the switch will cause noise to the entire system. As a result, the capacitor C<sub>1</sub> is used as a suitable decoupling (Mahesh et al., 2014). In this design, the buck converter is selected to operate at Continuous Conduction Mode (CCM). By using this method, the general performance of the converter will be suited to produce the maximum output power.

In this paper controllable voltage switch (MOSFET) with switching frequency up to (15kHz) was used, because it is more appropriate to the high frequency converters and for low power applications. The suitable selection of filter inductor for high frequency applications is the (toroidal type), its value can be calculated as in eq. (8) (Jianbo et al., 2013),

$$L = \frac{(1-D) V_O}{2 \times f \times I_O} \quad 8$$

Where, I<sub>o</sub>, V<sub>o</sub> are the output current and voltage respectively and (f) switching frequency. The power diode selection depends on its ability to face the output voltage of PV system specially at high switching frequency. Finally, the accurate calculation of output capacitor value assists

to avoid the ripple at output voltage. So, the output capacitor can be calculated in eq. (9) (Jianbo et al., 2013):

$$C_2 = \frac{(1-D) V_o}{2 \times f^2 \times L \times \Delta V_o} \quad 9$$

The value of input decoupling capacitor can be calculated in eq. (10) (Mahesh et al., 2014),

$$C_1 = I_o \times \frac{D(1-D)}{f \times \Delta V_{in P-P}} \quad 10$$

Where,  $\Delta V_o$  output voltage ripple,  $V_{in p-p}$  input peak to peak ripple voltage. The results of values calculated for different elements used in the buck converter design are presented in Table 2.

**Table 2. Parameters of Buck Converter.**

Elements		Values
MOSFET Transistor	Internal Resistance	0.1 ( $\Omega$ )
	Internal Diode Resistance	0.01 ( $\Omega$ )
	Switching frequency	15 (kHz)
Decoupling Capacitor ( $C_1$ )		2.76 (mF)
Inductor Filter (L)		$268 \times 10^{-2}$ (mH)
Capacitor Filter ( $C_2$ )		126 ( $\mu$ F)
Inductor current ripple ( $\Delta I$ )		30%
Output voltage		700 (V)

#### 4.2. MPPT Controller

The MPPT algorithm that was adopted in this system is the technique of Proportional/Integral (PI) controller. The Simulink circuit of MPPT with PI controller is illustrate in Fig. 7.

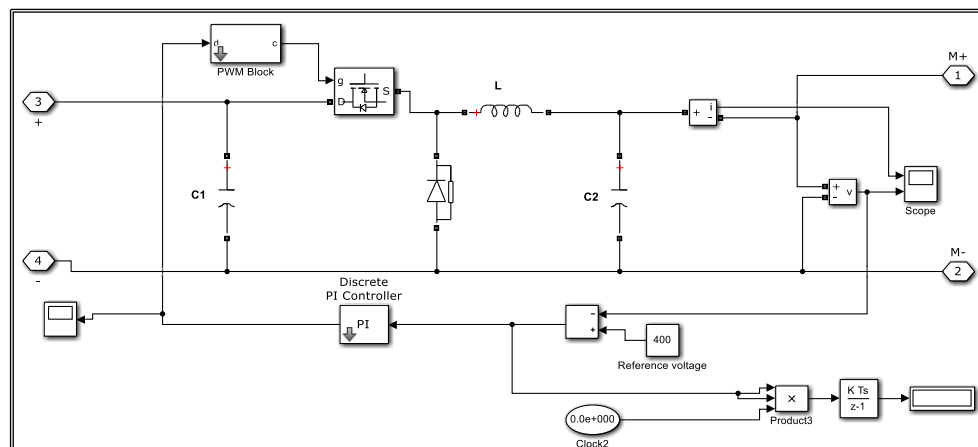


**Fig. 7. The Simulink circuit of MPPT control.**

The error signal  $V_e(t)$  is produced by comparing, the reference voltage signal which is generated from the MPPT with the PV voltage ( $V_{pv}$ ). The (PI) controller will process the error signal in order to produce an output signal  $U(t)$  which can be calculated by eq. (11), (12) (Dinesh and Sathish, 2015):

$$U(t) = K_P V_e(t) + K_i \int V_e(t) dt \quad 11$$

$$U(t) = K_P \left( V_e + \frac{1}{t_r} \int_0^t V_e(t) dt \right) \quad 12$$

Where,  $K_P$  and  $K_i$ , are the proportional and integral gains respectively, and  $t_r$  is the reset time.

The operating signal comprises of proportional error signal with integrated error signal. When PV power equips the buck converter, the PI controller starts to regulate the duty cycle values that will change the sensed input through the PI controller. Therefore, the values of proportional gain ( $K_P$ ) and integral gain ( $K_i$ ) constitutes a decisive factor to achieve a system with fast response. In this design, the values which are adopted according to trial and error method for the proportional and integral gains are ( $K_P = 0.1$  and  $K_i = 1$ ) respectively. The function of the proportional gain is to provide the system with fast error response, while the integrator gain leads the system to a steady-state error.

### 4.3. Storage Unit

The goal of using the storage unit is to supply necessary real power to generate compensation voltage, which protects nonlinear loads from shutdown or momentary interruption due to the voltage sags. This design used (Super High Energy Nickel-Metal-Hydride) batteries type due to many of advantages as: can be recharged hundreds of times, efficient at high rate discharges, operational life up to (2 years), and operates skillfully at a wide range of temperatures (-20 to 60° C) in charging and discharging (Saft batteries data sheet, 2011). The batteries will be charged from the PV via the circuit battery charger that is clarified in (Mano and Bhuvanesh, 2015). The value of DC voltage can be calculated by eq. (13) (Mano and Bhuvanesh, 2015),

$$V_{DC} = \frac{\sqrt{3} \times V_{M.Ph} \times \cos \vartheta}{\pi} \quad 13$$

Where,  $V_{M.Ph}$ . Maximum phase voltage,  $\vartheta$  the delay angle equal to zero. The battery parameters adopted are listed in Table 3, (Jianbo et al., 2013).

Table 3. Parameters of the Batteries.

Nominal voltage	Rated capacity	Maximum capacity	Full charge voltage	Discharge current	Internal resistance	Temp. range
700 (Volts)	30 (Amp.-hor.)	35.6 (Amp.-hor.)	720.5 (Volts)	10 (Amp.)	0.022 (Ohms)	-20 to 60 (°C)

## 5. SIMULATION AND RESULTS

The obtained results in this design are fully achieved by using MATLAB/ 'Simulink'. These results include waveforms of the voltage source, the DVR voltage, the load voltage, and the Total Harmonic Distortion (THD) of the load voltage during the voltages of sag/swell. In addition to the waveforms of the PV array, MPPT and the battery output. The simulation parameters specifications which employed are, discrete with simulation time 800 millisecond and the sampling time  $20e^{-6}$  second. The non-linear load consists of RL series load connected with full-bridge inverter to feed ( $R= 62 \Omega$  and  $L= 0.15$  mH) load. Fig.8 illustrates the complete simulated circuit for proposed design.

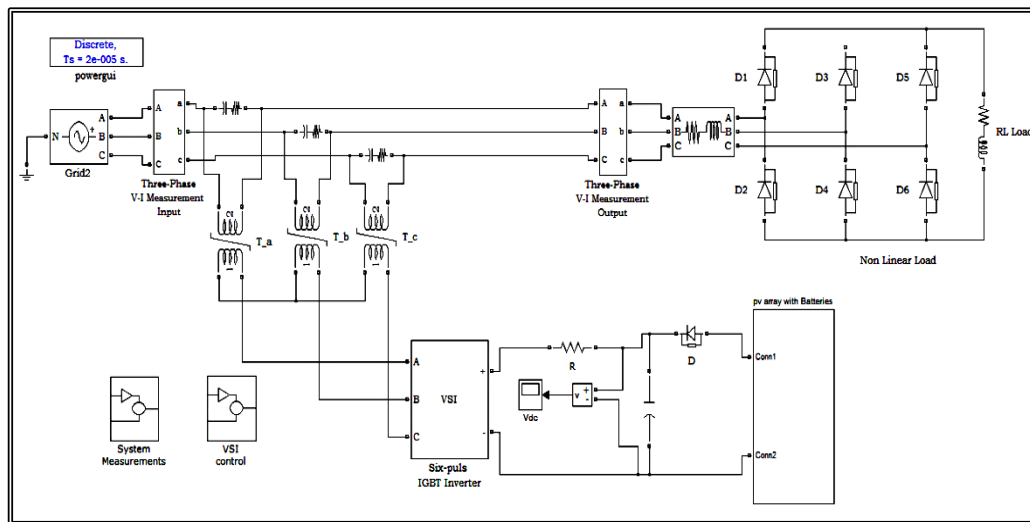
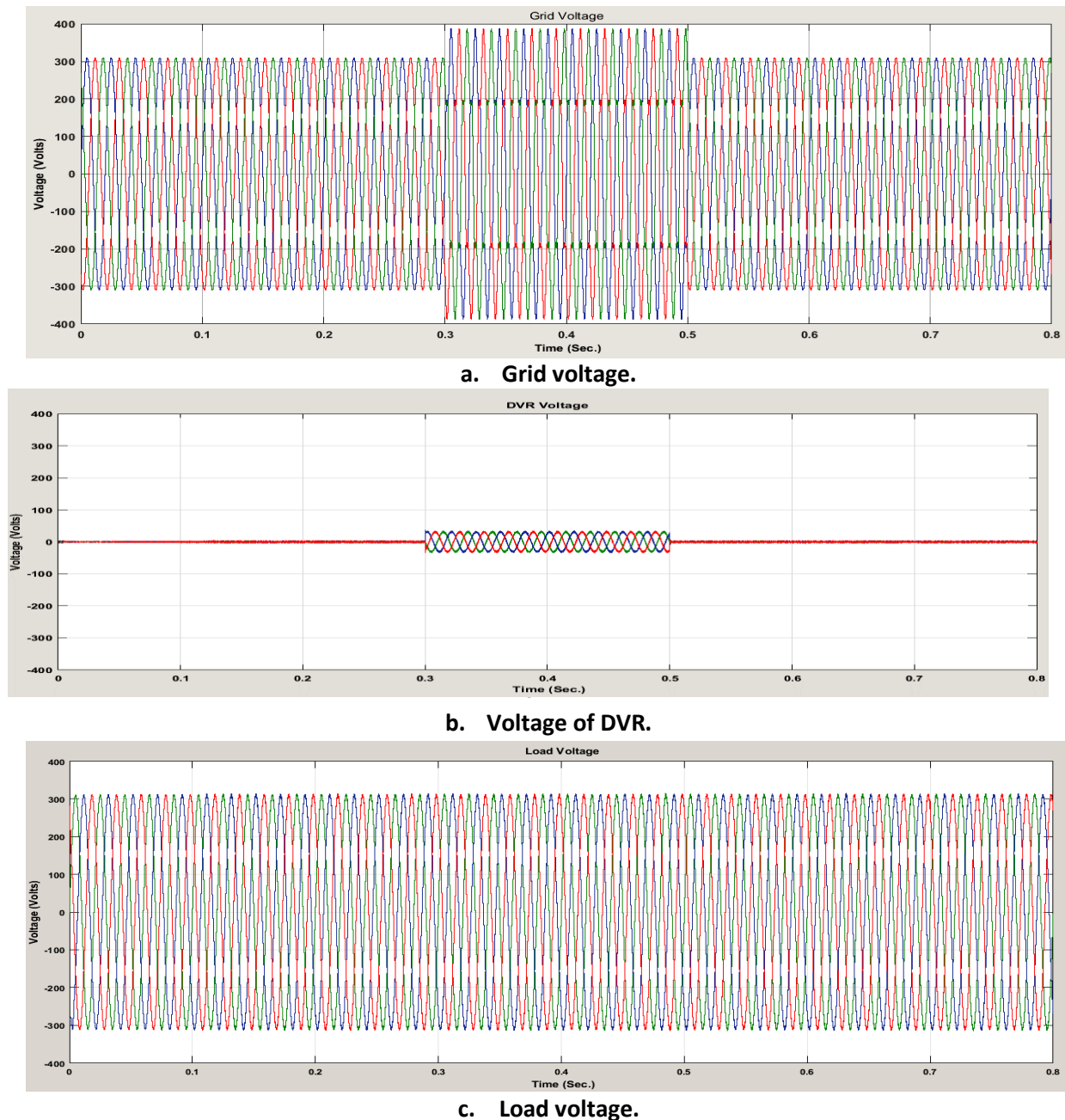


Fig. 8. Complete simulation circuit of proposed design.



**Fig. 9. Voltages waveform of proposed system at voltage swell.**

As demonstrated in Fig. 9-a, the value of voltage swells at grid reached to 50 V higher than source voltage for a while of 200 milliseconds; from (300 to 500 millisecond). While, Fig.9-b; reveals the performance of DVR in detection and amendment for voltage swell, with same value and duration for disturbance voltage. Fig.9-c, illustrate the load voltage after improvement where, there is no existences for any effect to the transient's during the voltage injection.

According to analysis of Fast Fourier Transform (FFT), Total Harmonic Distortion (THD) of the load voltage during the DVR work equate 0.77%, as exemplified in Fig. 10.

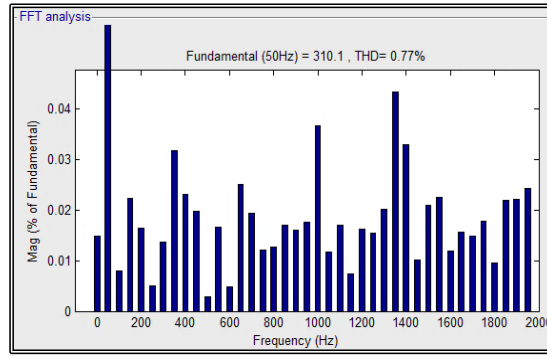
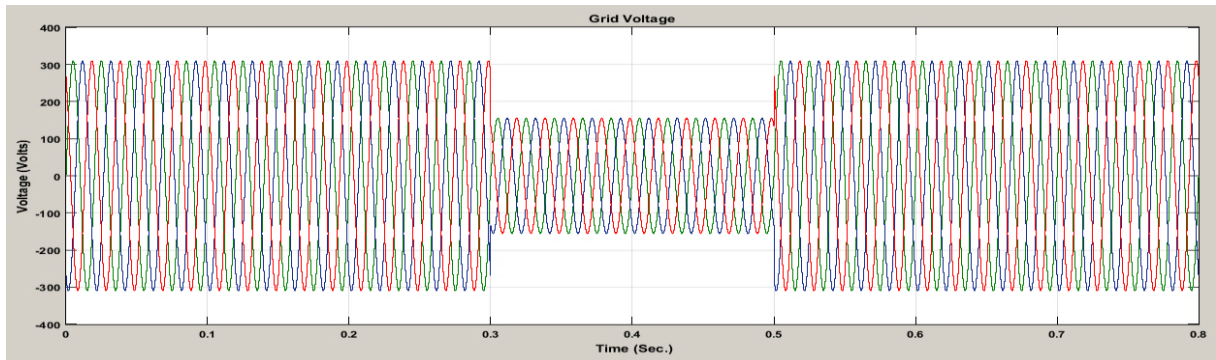
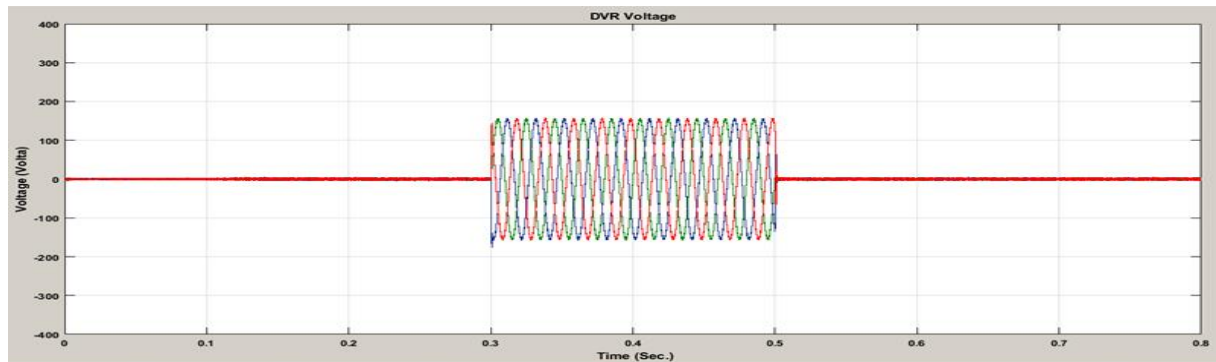


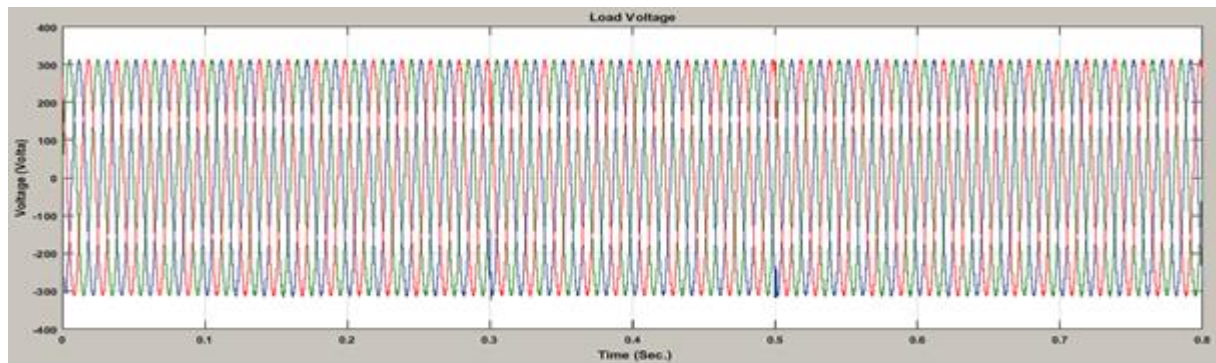
**Fig. 10. THD analysis of load voltage during voltage swells.**



**a. Grid voltage.**



**b. Voltage of DVR.**



**c. Load voltage.**

**Fig. 11. Voltages waveform of proposed system at voltage sag.**

As demonstrated in Fig. 11- a, the value of voltage sag at grid reach to 110 V lower than supply voltage for continue to 200 milliseconds; from (300 to 500 millisecond). While, Fig.11-b; reveals the performance of DVR in detection and compensation for sag voltages, the same value and duration of a disturbance voltage. The load voltage after compensation is illustrated in Fig.11-c.

The (THD) of the load voltage during the DVR work equate 0.77%, as exemplified in Fig. 12. The output of maximum power is tracked to the corresponding irradiation, as displayed in Fig. 13. The value of DC voltage that feeds into DVR is 380 V, as displayed in Fig. 14.

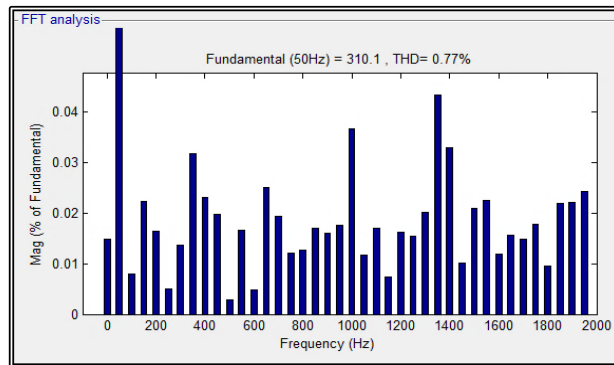


Fig. 12. THD analysis of load voltage during voltage sag.

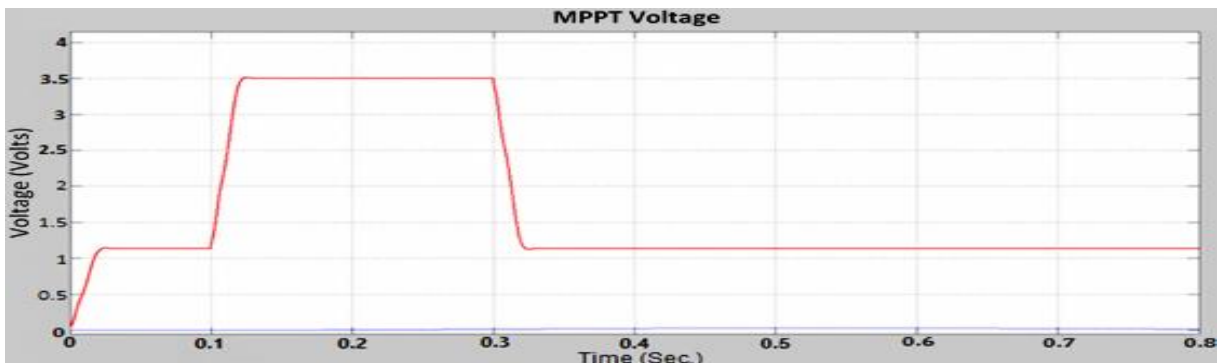


Fig. 13. Voltage of MPPT with PI control.

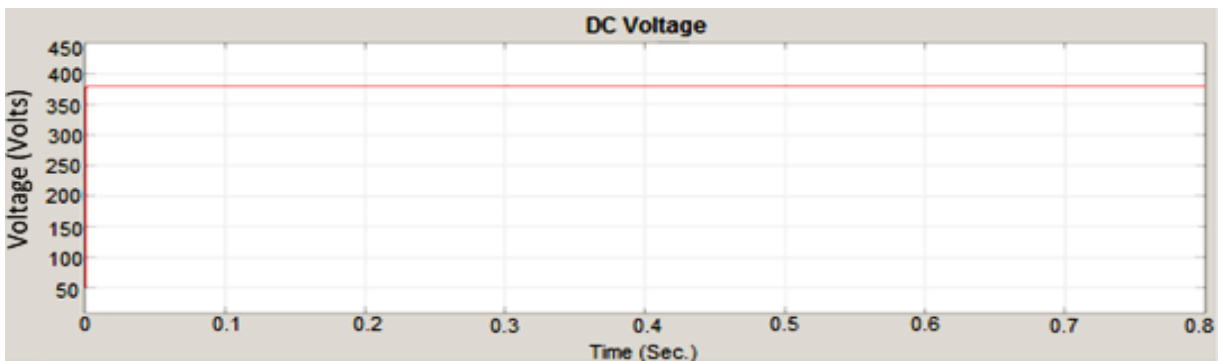
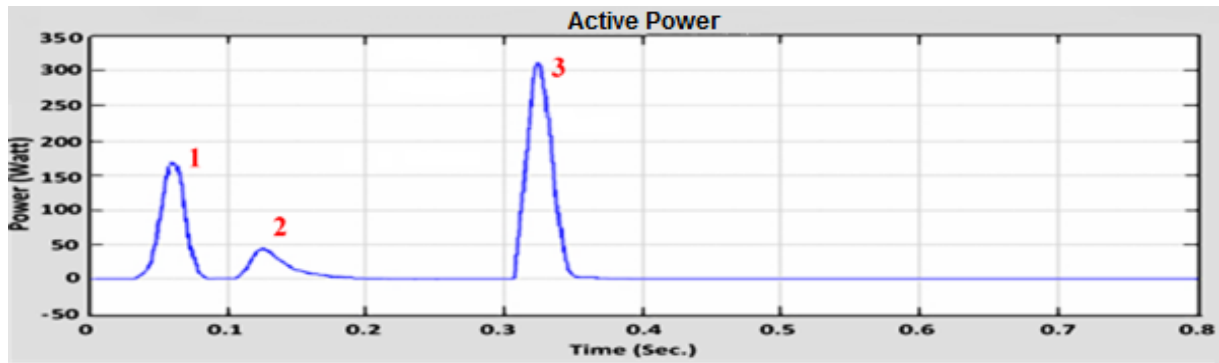


Fig. 14. DC voltage that feeds into DVR.



**Fig. 15. The active power of PV module.**

As displayed in Fig. 15; the first and second peak values of active power illustrate the effect of solar radiation change on PV module and function of the MPPT. While, the third peak value indicate to the active power associate with DVR action. In other words, the maximum power supplied to the DVR at the moment of disturbances occurred.

The current value that drawn from battery is 0.62 A at typical operation, while increasing to 1.2 A as soon as disturbance occurs, as displayed in Fig. 16.

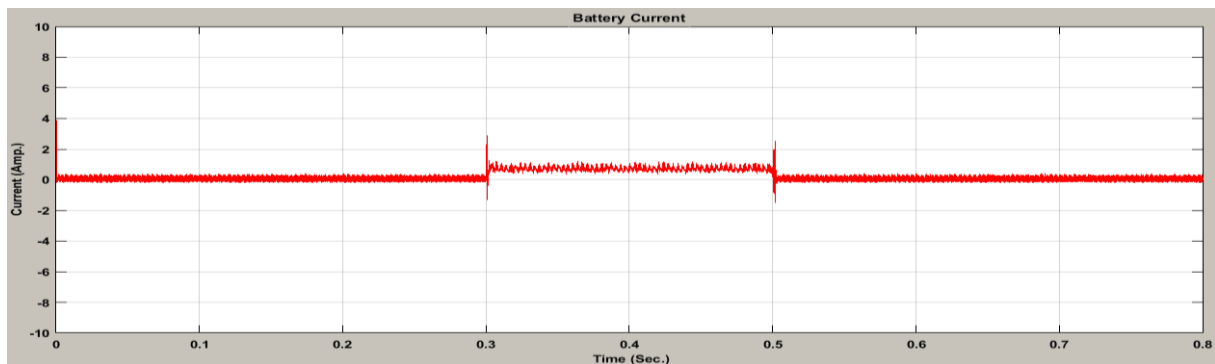


**Fig. 16. Battery current provided the DVR.**

## 6. CONCLUSIONS

Simulation results illustrate the fast dynamic response and high reliability to detect and protect the critical loads from voltage sag and swell. Based on this development, the system characterized by the stability of performance before and during the occurrence of disturbances, complete absence of the effect of transients. The results also exhibited the effectiveness of MPPT to maintain voltage that is provided to the DVR a stable under different conditions for radiation change and electrical grid disturbances.

## **7. REFERENCES**

- Apinan A. and Worawat S. (2008) 'Synchronization Technique for Random Switching Frequency Pulse-Width Modulation', *International Journal of Electrical, Computer, Energetic, Electronic and Communication Engineering*, 2(3): 384-389.
- Canadian Solar Inc. (2016) 'PV Module Product Datasheet of The CS6X-310', Canadian Solar, V5.4C1\_EN, available: ([http:// www.canadiansolar.com](http://www.canadiansolar.com)).
- Chandani S. and Jain A. (2014) 'Maximum Power Point Tracking Techniques: A Review', *International Journal of Recent Research in Electrical and Electronics Engineering*, 1(1), 25-33.
- Dawn Ph. and Samina T. (2016) 'Dynamic Voltage Restorer Based On Hysteresis Voltage Control for Voltage Sag Mitigation and Harmonics Elimination', *International Journal of Scientific Development and Research*, 1(10), 11-13.
- Dinesh M., Venkatesan K. and Baskaran J. (2015) 'Design, Control and Simulation of Buck Converter using PID controller and Reference Regulator Technique', *International Journal on Recent Technologies in Mechanical and Electrical Engineering*, 2(10), 58-62.
- Dinesh M. and Sathish K. (2015) 'Design and Control of Buck Converter using PI control and Reference Regulator Technique', *International Journal on Recent Technologies in Mechanical and Electrical Engineering (IJRMEE)*, 2(3), 046 – 049.
- Jianbo Y., Weiping Z., Faris Al-Naemi<sup>1</sup>, and Xiaoping Ch. (2013) 'A High Power Factor Rectifier Based on Buck Converter Operating in Discontinuous Inductor Current Mode', *An Academic Publisher Journal of Power and Energy Engineering Scientific Research*, 5 (4B), 842-849.
- Kalaivani R., Arunvishnu K., Jakir M., Lokesh R. and Rajkumaran M., (2016) 'Elimination of Voltage Sag/Swell Using Dynamic Voltage Restorer', *International Journal for Research in Technological Studies*, 3(4): 37-41.
- Mahesh G., Yadu K. and Parthasarthy S. (2014) 'Modelling of Buck DC-DC Converter Using Simulink', *International Journal of Innovative Research in Science-Engineering and Technology*, 3(7), 14965- 14975.
- Mano P. and Bhuvanesh A., (2015) 'Design and Implementation of Battery Charger Using Flyback Converter for Constant Current and Voltage Control', *International Journal for Research in Applied Science & Engineering Technology*, 3(1), 153-159.

Nagesh R., and Rajendra M., (2016) 'An Overview on SVPWM Control Technique Used in DVR', *International Journal of Engineering Research & Technology*, 5(3), 192- 194.

Prachi S. and Gaurav N., (2013) 'Analysis and Hardware Implementation of Three-Phase Voltage Source Inverter', *International Journal of Engineering Research and Technology*, 2(5), 2209-2218.

Sanjay H. and Gaurav G., (2013) 'Mitigation of Voltage sag/swell Using Dynamic Voltage Restorer ', *Journal of Electrical and Electronics Engineering*, 8(4), 21-38.

Roger C., Mark F., Surya Santoso and H. Wayne, (2012) 'Electrical Power Systems Quality', 3rd Edition, McGraw-Hill Companies, United States of America.

Yogita H., Hardik M. and Bharti B., (2016) 'Analysis and Simulation of Voltage Sag/ Swell of A Distribution System without and with Dynamic Voltage Restorer', *International Journal of Engineering Development and Research*, 4(2), 704-710.

Sanjay M. and Gaurang C., (2015) 'Control of Series Active Power Filter for Improvement of Power Quality ', *Journal of Emerging Technologies and Innovative Research*, 2(4): 992-996.

Sathish, A., Raghu T. and Chandra S., (2015) 'Fault Current Interruption by the Simplified Dynamic Voltage Restorer to Enhancing Power Quality', *International Journal of Emerging Trends in Electrical and Electronics*, 11(3), 16-20.

Saft batteries data sheet, France, (2011) 'Super High Energy Nickel-Metal Hydride Battery System', The Communication Department, DOC N°11123-2-1109, available: <http://www.saftbatteries.com>.

Sangita R., and Mini R., (2014) 'Modeling Simulation and Design of Photovoltaic Array with MPPT Control Techniques', *International Journal of Applied Power Engineering*, 3(1), 41-50.

Saravana, S. and Pratap, N., (2016) 'A Review on Photo Voltaic MPPT Algorithms', *International Journal of Electrical and Computer Engineering*, 6(2), 567-582.

Shilpashinde and Kelapure R., (2016) 'A Novel Dynamic Voltage Restorer', *International Journal of Innovations in Engineering Research and Technology*, 3(5), 59-64.